

## **General Disclaimer**

### **One or more of the Following Statements may affect this Document**

- This document has been reproduced from the best copy furnished by the organizational source. It is being released in the interest of making available as much information as possible.
- This document may contain data, which exceeds the sheet parameters. It was furnished in this condition by the organizational source and is the best copy available.
- This document may contain tone-on-tone or color graphs, charts and/or pictures, which have been reproduced in black and white.
- This document is paginated as submitted by the original source.
- Portions of this document are not fully legible due to the historical nature of some of the material. However, it is the best reproduction available from the original submission.



## Technical Memorandum 78046

# Satellite Doppler Data Processing Using A Microcomputer

**P. E. Schmid and J. J. Lynn**

(NASA-TM-78046) SATELLITE DOPPLER DATA  
PROCESSING USING A MICROCOMPUTER (NASA)  
62 p HC A04/MF A01 CSCL 22A

N78-17130

Unclas  
G3/15 05047

**DECEMBER 1977**

National Aeronautics and  
Space Administration

**Goddard Space Flight Center**  
Greenbelt, Maryland 20771



**SATELLITE DOPPLER DATA  
PROCESSING USING A  
MICROCOMPUTER**

**P. E. Schmid**

**Goddard Space Flight Center  
Greenbelt, Maryland 20771**

**J. J. Lynn**

**Old Dominion Systems, Inc.\*  
Gaithersburg, Maryland 20760**

**December 1977**

**\*Microcomputer development under NAS5-23587.**

**GODDARD SPACE FLIGHT CENTER  
Greenbelt, Maryland**

# **SATELLITE DOPPLER DATA PROCESSING USING A MICROCOMPUTER**

**P. E. Schmid**

**Goddard Space Flight Center**

**Greenbelt, Maryland 20771**

**J. J. Lynn**

**Old Dominion Systems, Inc.**

**Gaithersburg, Maryland 20760**

## **ABSTRACT**

This paper describes a microcomputer which was developed to compute ground radio beacon position locations using satellite measurements of Doppler frequency shift. Both the computational algorithms and the microcomputer hardware incorporating these algorithms are discussed. Results are presented where this microcomputer in conjunction with the NIMBUS-6 Random Access Measurement System (RAMS) provides real-time calculation of beacon latitude and longitude.

## CONTENTS

	Page
ABSTRACT .....	iii
1.0 INTRODUCTION.....	1
2.0 SYSTEM DESCRIPTION.....	2
3.0 COMPUTATIONAL ALGORITHMS.....	6
3.1 A Priori .....	8
3.2 Ambiguity Resolution.....	11
3.3 Atmospheric Effects.....	17
3.4 Orbit Update Procedure.....	22
3.5 Error Sources.....	25
4.0 MICROCOMPUTER DESCRIPTION.....	28
4.1 Central Processing Unit .....	29
4.2 Data and Program Memory.....	34
4.3 Input-Output Peripherals.....	35
5.0 NIMBUS-6 RESULTS .....	38
6.0 CONCLUSIONS.....	40
APPENDIX — LEAST SQUARES MICROCOMPUTER ALGORITHM.....	41
ACKNOWLEDGEMENT.....	53
REFERENCES.....	54

## ILLUSTRATIONS

Figure		Page
1	Beacon-To-Satellite Geometry .....	3
2	Typical One Way Doppler Measurement .....	5
3	Overall System .....	7
4	Simplified Solution Using Point of Closest Approach .....	10
5	Earth Rotation Effect (0° Latitude) .....	14
6	Earth Rotation Effect (30° Latitude).....	15
7	Earth Rotation Effect (60° Latitude).....	16
8	Basic Position Location Microcomputer and Interface.....	30
9	Position Location Microcomputer.....	36
10	Microcomputer Printed Circuit Cards.....	36
11	Typical Position Location Results .....	39

## 1.0 INTRODUCTION

A well established application of near Earth orbiting satellites is the task of data collection and distribution. If the data is relayed in real-time the collection area is limited to the satellite field of view. For a nominal polar orbiting 1000 km altitude satellite such as NIMBUS-6, this corresponds to a maximum coverage circle of approximately 6000 km in diameter. Since the orbital period is on the order of 110 minutes worldwide coverage is obtained at least every 13 orbits. If the data is stored onboard by means of a tape recorder and "dumped" on command to the interrogating station, coverage is limited only by ground beacon deployment. NIMBUS-6 can operate in both onboard storage and real-time data relay modes. In either case the data format seen by the ground processing computer is the same.

Ever since launch (June 12, 1975) NIMBUS-6 has been relaying data from a number of platforms associated with meteorological monitoring balloons and buoys (Ref. 1, 2, 3). In these applications platform location as well as platform data (for example, temperature and pressure) are required. The microcomputer discussed in this paper has been evaluated by using both taped data as well as tying in directly to equipment capable of receiving and demodulating real-time NIMBUS-6 telemetry and RAMS Doppler frequency data. The telemetry decommutation is rather straightforward and will not be discussed at length. The Doppler processing for purposes of beacon position determination is considerably more complex and it is this aspect of the microcomputer which will be discussed in detail. The same computer technology is directly applicable to

forthcoming missions such as the near Polar orbiting TIROS-N Satellite Aided Search and Rescue demonstration. This TIROS-N demonstration, which is scheduled to begin in early 1981, will relay the Doppler shifted signal from low power "distress beacons" at 121.5, 243 and 406 MHz. In a manner analogous to the NIMBUS-6 buoy tracking, the ground based computer will combine the Doppler information with known satellite orbit information to compute the latitude and longitude of the "distress beacon" (Ref. 4, 5, 6).

## 2.0 SYSTEM DESCRIPTION

The radio beacon-to-satellite geometry is as indicated in Figure 1. As will be shown, the use of geocentric Earth fixed coordinates greatly simplifies the computational problem. In such a coordinate system the range  $R$ , and its time derivative  $\dot{R}$  can be expressed as:

$$R^2 = (X - S_1)^2 + (Y - S_2)^2 + (Z - S_3)^2 \quad (1)$$

$$\dot{R} = \frac{\partial R}{\partial X} \dot{X} + \frac{\partial R}{\partial Y} \dot{Y} + \frac{\partial R}{\partial Z} \dot{Z} = \frac{(X - S_1)}{R} \dot{X} + \frac{(Y - S_2)}{R} \dot{Y} + \frac{(Z - S_3)}{R} \dot{Z} \quad (2)$$

In practice a constant bias term must also be included in equation 2 to account for frequency offset. This offset is solved for along with the beacon position. The beacon coordinates  $S_1, S_2, S_3$ , are easily transformed to longitude and geodetic latitude. The satellite coordinates  $X, Y, Z$  and corresponding velocity components  $\dot{X}, \dot{Y}, \dot{Z}$ , being "Earth Fixed" inherently include the effect of Earth rotation which is on the order of  $7.3 \times 10^{-5}$  radians/sec.

In the NIMBUS-6 Rams system the beacon is self timed and transmits at a nominal 401.2 MHz once per minute for a one second period. The one second

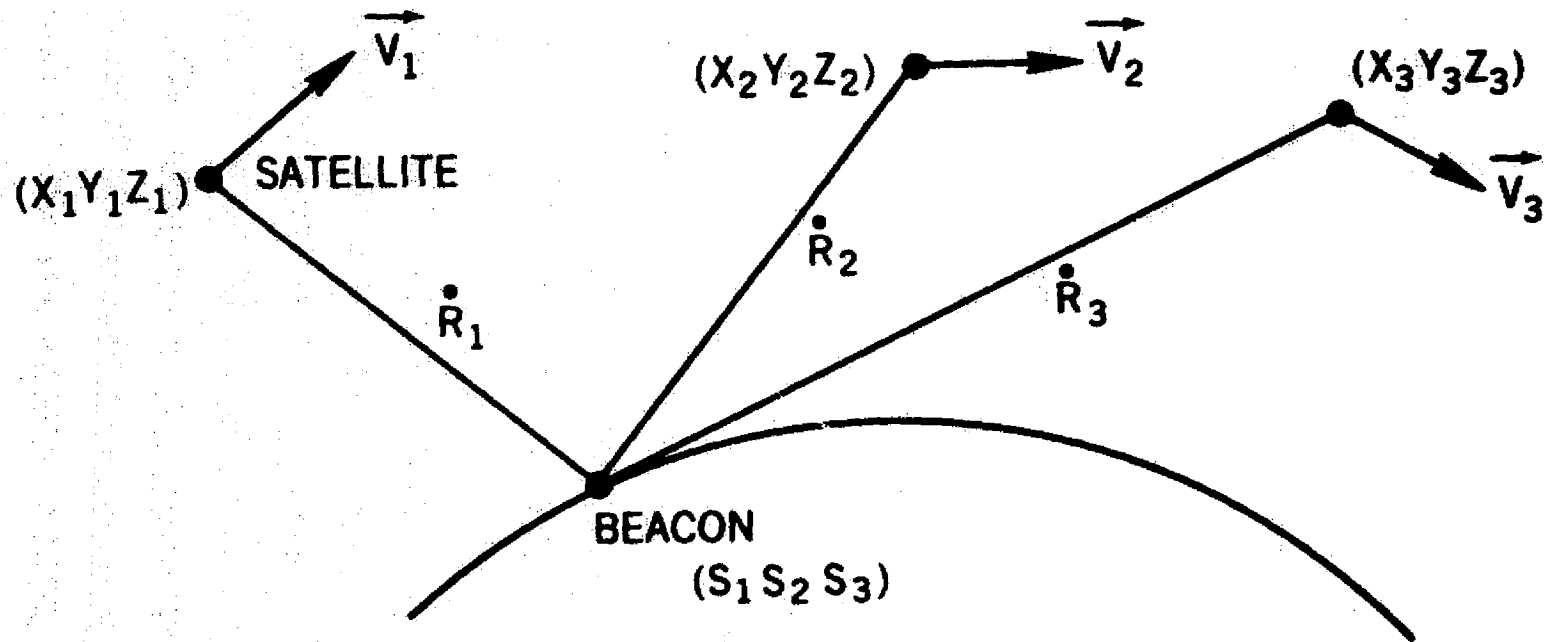


Figure 1. Beacon-To-Satellite Geometry

transmission includes 320 milliseconds of unmodulated carrier followed by 640 milliseconds of PSK modulated digital data at a 100-bps data rate. For position location purposes NIMBUS-6 measures the uplink Doppler shifted frequency associated with the unmodulated carrier. With reference again to Figure 1, the range rate,  $\dot{R}$ , is related to the one way Doppler shifted signal by:

$$f = -\frac{\dot{R}}{C} f_T \quad (3)$$

where for NIMBUS-6 RAMS:

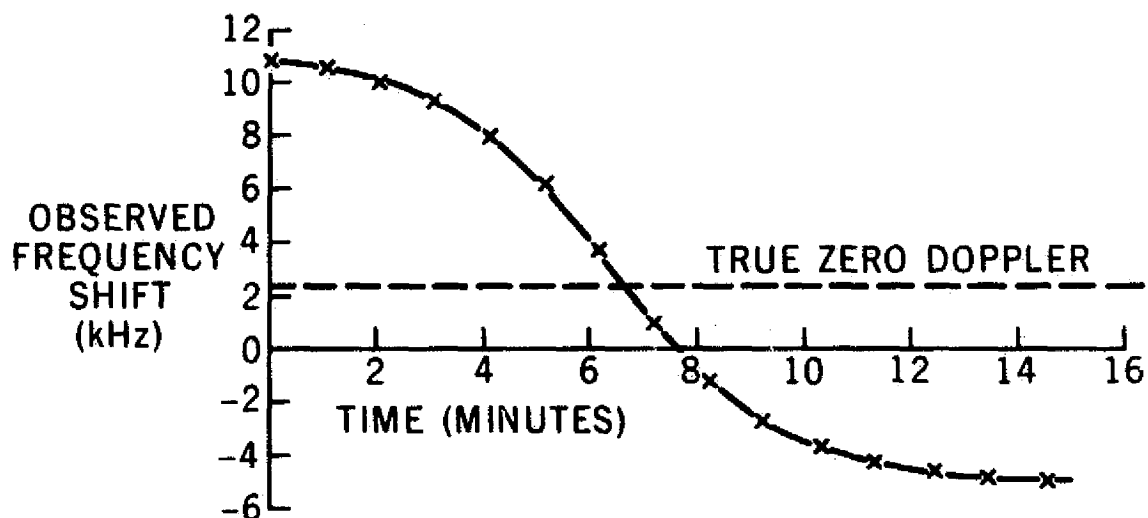
$f_T$  = beacon transmit frequency = 401.2 MHz

$\dot{R}$  = beacon-to-satellite range rate  $-7 \text{ km/sec} < \dot{R} < 7 \text{ km/sec}$

$C$  = speed of light  $\approx 3 \times 10^5 \text{ km/sec}$

As a consequence of this Doppler shift and the frequency tolerance ( $\pm 5 \text{ KHz}$ ) of the platform crystal oscillators, the NIMBUS-6 receives a signal somewhere in a band of  $\pm 15 \text{ KHz}$ . This frequency dispersion allows the RAMS system to track up to 200 beacons during any given satellite pass. Additionally each beacon is identified by a unique ID. The ID uses 12 bits of the 64 bits of data transmitted once per minute. Since the transmit frequency of the remote beacon is seldom known to better than a few KHz, the position location algorithm must accurately determine this frequency (or equivalently range rate) bias in order to compute beacon latitude and longitude. Experience has shown that the computer can recover this frequency bias to a high degree of accuracy (i.e. to better than a few Hz) even though data from the Doppler curve's point of inflection is excluded. Figure 2 indicates a typical NIMBUS-6 Doppler pass. The recovered frequency bias in this particular case was on the order of 2 KHz. The ordinate

## TYPICAL ONE WAY DOPPLER MEASUREMENT



NOTE: FAIRBANKS STATION TO NIMBUS-6

$f_0 = 401.2$  MHz

START TIME 10 AUGUST 1975

21 H 12 M 31.44 S

Figure 2. Typical One Way Doppler Measurement

labeled "true zero Doppler" corresponds to the time when the beacon-to-satellite distance was a minimum. It should be reiterated, however, that as a consequence of the least squares algorithm discussed in this paper, Doppler data in the region of closest approach is not a requirement for frequency bias recovery.

The overall system configuration used during the microcomputer evaluation is shown in Figure 3. The ground terminal is a NASA prototype of a fully automated NIMBUS-6/TIROS-N data collection station. For TIROS-N tracking the azimuth/elevation antenna drive will be directed by the same microcomputer which provides platform position location and telemetry data readout.

### 3.0 COMPUTATIONAL ALGORITHMS

The algorithms presented herein apply strictly to stationary platforms. Any platform motion will of course modify the Doppler signature and if this motion is left unmodeled a position location error will result. For slowly moving platforms such as drifting buoys this error is small and position determinations from successive passes can be used to estimate drift velocity.

The error due to unmodeled platform motion can be shown to be on the order of 0.2 km per km/hour of uncorrected speed. At present the microcomputer is programmed to provide beacon latitude and longitude based on either a single pass or two successive satellite passes of Doppler data. For the single pass solution a minimum of 3 Doppler measurements are required since 3 unknowns (latitude, longitude and frequency bias) are solved for. Since the RAMS Doppler data rate is one measurement per minute, a maximum of approximately 15 data points per pass can be expected. Any additional information such as in situ observations of platform heading or speed, if sent back to

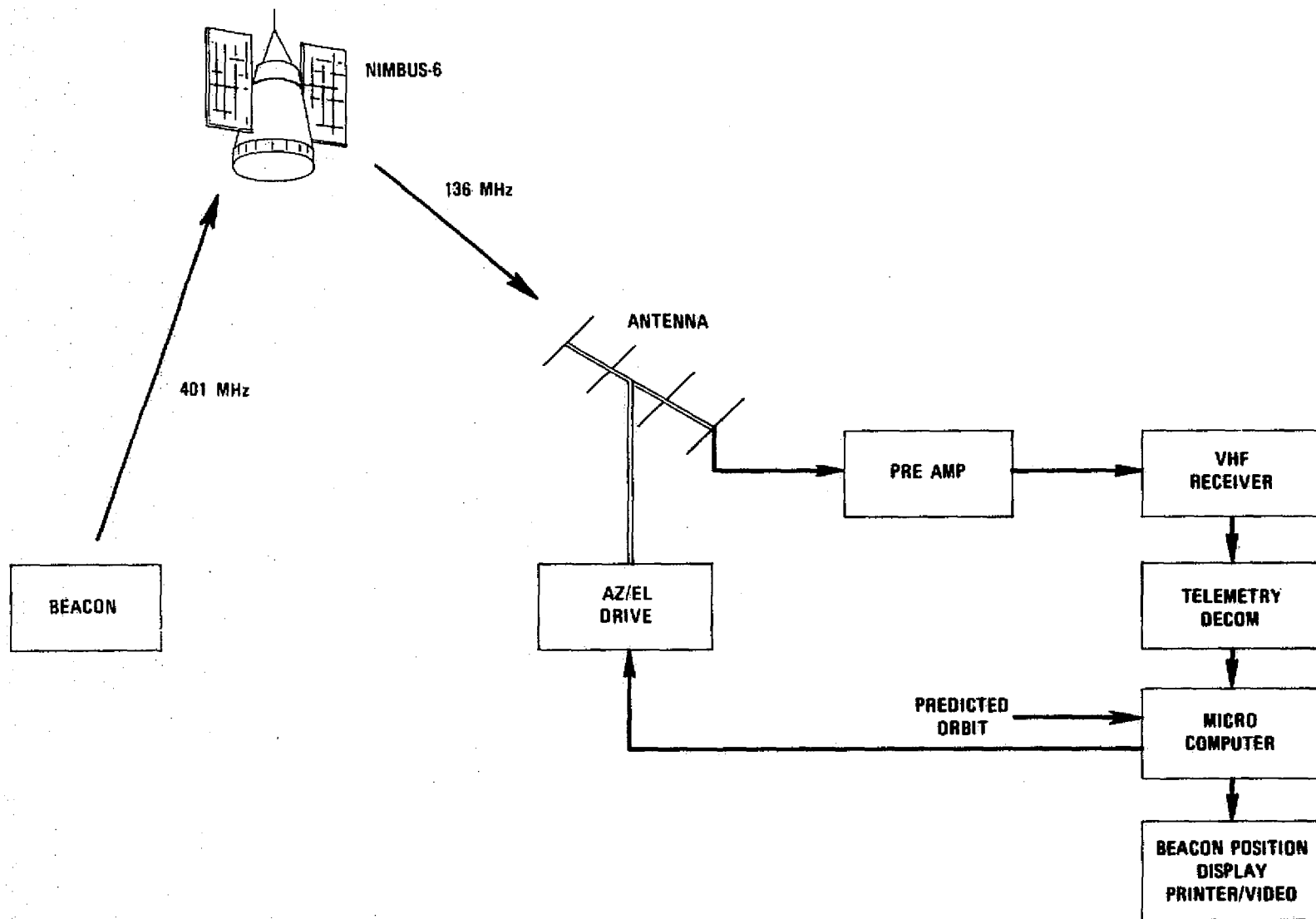


Figure 3. Overall System

the microcomputer, can be used to construct a complete time history of position location over the pass interval.

### 3.1 A Priori

An "A Priori" or "first guess" of position location must be used as a starting point for any least squares type of algorithm. The better the initial estimate the fewer the number of iterations required to obtain a converged solution. In many cases such as that of a drifting buoy a previous position determination is the obvious choice for a first guess. However, there are cases when no prior beacon positions are available. One such application is satellite aided search and rescue where the beacon is associated with a downed aircraft.

In this case, one straightforward approach which works well is simply to let the computer scan a grid of the Earth surface in view of the satellite during the Doppler data collection interval. Each point on the grid is used successively as a starting value for the least squares algorithm until one that gives convergence is obtained. Another useful starting position is taken to lie on a great circle on the Earth's surface perpendicular to the ground track of the satellite at the midpoint of the pass. The point on the great circle is selected at some arbitrary location between the ground track and the radio horizon. If data is collected during the time of closest approach (TCA) the following equations can be solved to obtain an estimate of beacon position:

$$S_1^2 + S_2^2 + S_3^2 = a^2 \quad (4)$$

$$\dot{X}S_1 + \dot{Y}S_2 + \dot{Z}S_3 = \dot{X}X + \dot{Y}Y + \dot{Z}Z \quad (5)$$

$$XS_1 + YS_2 + ZS_3 = \frac{1}{2} \left[ a^2 + \rho^2 - R_{\min}^2 \right] \quad (6)$$

A spherical Earth is used in this approximation with the geometry indicated in Figure 4. The satellite coordinates are Earth fixed geocentric and hence include Earth rotation. The beacon-to-satellite range at time of closest approach can be approximated (Ref. 7) neglecting the effect of Earth rotation by:

$$R_{\min} = \frac{-\rho^2 \ddot{R}}{V^2} + \left[ \frac{\rho^4 \ddot{R}^2}{V^4} + \rho^2 + a^2 \right]^{1/2} \quad (7)$$

where:

$a$  = Earth radius

$V$  = satellite speed

$h$  = satellite height

$\rho = a + h$

$$\ddot{R} = -\dot{f}_d \frac{c}{f_T}$$

and

$\dot{f}_d$  is the slope of Doppler curve at TCA (i.e. maximum slope of Doppler curve)

Inspection of equations 4, 5, and 6 indicate the intersection of two planes (a straight line) in turn intersecting a sphere. The two single pass solutions thus obtained are approximations to the true and to the so called "image" solution. In the absence of Earth rotation the two solutions would be indistinguishable. Separation of these two solutions on the basis of Earth rotation effects is discussed in the next section entitled "ambiguity resolution".

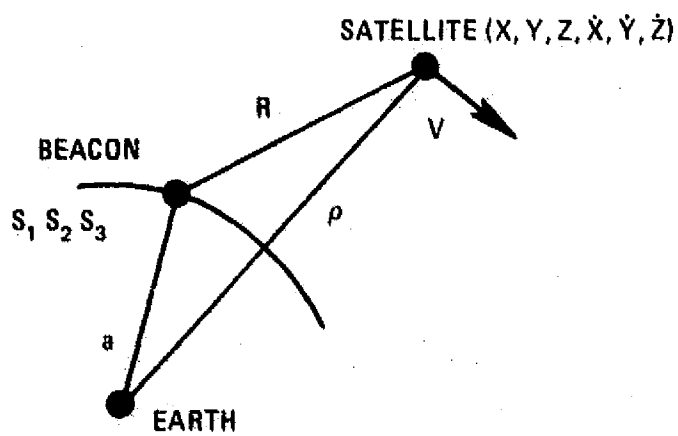


Figure 4. Simplified Solution Using Point of Closest Approach

Finally there are other more accurate but more complex approximations which directly solve the range-rate observational equation independent of the relative beacon-to-satellite geometry. Such schemes include the fitting of a high order polynomial to the data or fitting portions of the data with segments of parabolas. However, experience to date indicates that even a crude estimate, in error by several thousand km, will for most cases result in a converged least squares solution in 5 iterations or less. The time for computing a typical 10 point Doppler solution using 5 iterations on the present microcomputer is on the order of 2 minutes.

### 3.2 Ambiguity Resolution

For any given satellite pass and beacon-to-satellite geometry there will be two locations, each at the same orthogonal distance from the ground trace, where the range-rate (and hence Doppler shift) will be zero at TCA. While these 2 Doppler characteristic curves go through zero at the same time, because of Earth rotation the shape of the two characteristics will be slightly different. Hence the measured Doppler data will be best fitted by the calculated Doppler corresponding to the side of the true location. On a single satellite pass the true location can then be separated from the image location by comparing the RMS observed — minus-calculated residuals for each side. Simulations have shown that in the absence of data noise and in the presence of a well distributed data set this distinction is easily made. If two or more satellite passes of data are available this so called ambiguity is resolved simply from geometric considerations. Some insight into how Earth rotation affects the Doppler characteristics can be obtained by writing equations in terms of beacon latitude,  $\phi$ , and longitude,  $\lambda$ . As a further simplification assume a spherical Earth of radius 'a'

and a Polar orbiting satellite at height,  $h$ . The range-rate can then be expressed (Ref. 8) as:

$$\dot{R} = \frac{(a + h) a}{2R} \left\{ (\omega_s + \omega_e) \cos \phi \sin [(\omega_s + \omega_e) t + \lambda] + (\omega_s - \omega_e) \cos \phi \sin [(\omega_s - \omega_e) t - \lambda] - 2\omega_s \sin \phi \cos \omega_s t \right\} \quad (8)$$

where:

$\omega_e$  = Earth rotation rate  $\doteq 7.3 \times 10^{-5}$  radians/sec

$\omega_s$  = Satellite angular rate  $\doteq 10^{-3}$  radians/sec

$R$  = beacon-to-satellite slant range

The effect of Earth rotation is nearly orthogonal to satellite velocity at the equator and nearly collinear with satellite velocity at the poles. The difference between the image and true Doppler characteristics is thus a minimum at the equator and maximized at the poles. Equation 8 can be used to obtain an approximate analytic expression for this Doppler (range rate) characteristic difference,  $\delta \dot{R}$ , at the equator where  $\phi = 0$  and a circular polar orbit is again assumed with  $\lambda$  referenced to a TCA overhead satellite equator crossing at  $0^\circ$  longitude:

$$\delta \dot{R} = \frac{2a(a + h) \omega_s^2 \omega_e t^2 \sin \lambda}{[a^2 + (a + h)^2 - 2a(a + h) \cos \lambda \cos \omega_s t]^{\frac{1}{2}}} \quad (9)$$

where:

$\lambda$  = beacon longitude

$t$  = time relative to TCA

$\delta \dot{R}$  = true minus image characteristic

and all other symbols are as previously defined

As per equation (3) the frequency characteristic difference will depend on the beacon transmission frequency. A somewhat more general approach was taken via computer simulation and many computer plots of this effect for various satellite inclinations (i.e. including other than polar), latitudes of TCA, and beacon-to-satellite TCA elevation angles have been obtained. Figures 5, 6, and 7 indicate typical computer plots of the range rate difference due to Earth rotation for a satellite at 1000 km altitude, circular orbit and  $80^\circ$  inclination, and elevation angle at TCA of  $60^\circ$  at latitudes of  $0^\circ$ ,  $30^\circ$  and  $60^\circ$ . It should be noted that at the equator the maximum excursion is on the order of 25 meters/sec (33 Hz at 401.2 MHz) and at latitude  $60^\circ$  it is 140 meters/sec (190 Hz at 401.2 MHz). The times indicated in Figures 5, 6, and 7 are relative to TCA and run to the radio horizon for the given satellite pass. Since the observed Doppler noise on the 401.2 MHz RAMS system is typically 0.5 Hz, Earth rotation signatures are observable.

However, it should be pointed out that the degree of observability is also a function of the quantity of data collected. For example 3 Doppler data points at a one per minute rate near the beginning of the pass may be insufficient to allow image discrimination.

The real test, in the absence of a complete data span, is to generate a simulated "noisy" data set for one side of the pass and compute both solutions using the least squares algorithm and compare observed-minus calculated residuals. A number of such simulations have been run and indications are that even under somewhat marginal conditions of geometry and data quantity the true location can generally be separated from the ambiguous location on a single pass.

SATELLITE ORBIT INCLINATION = 80 DEGREES

LATITUDE OF BEACON = 0 DEGREES

TCA ELEVATION ANGLE = 60 DEGREES

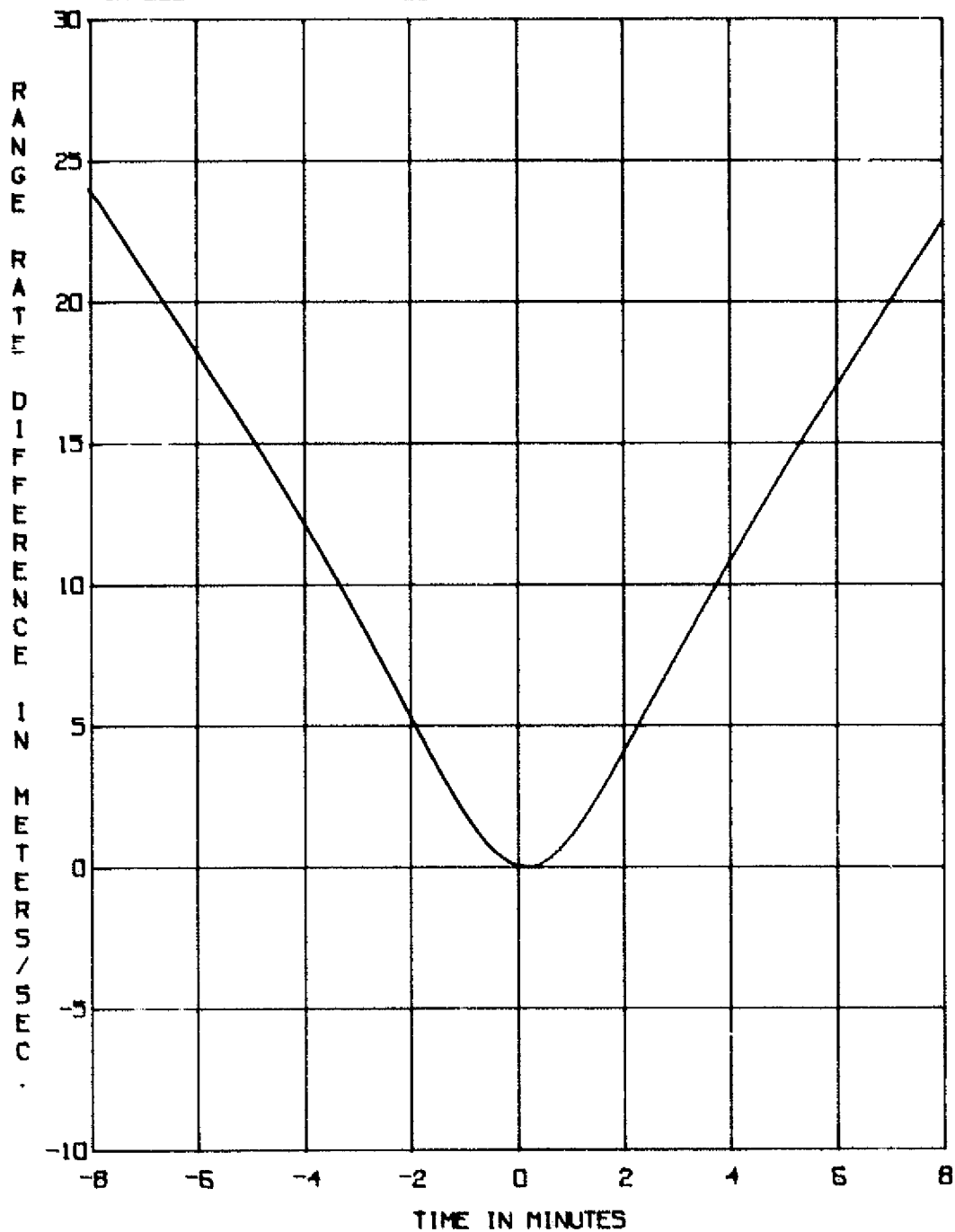


Figure 5. Earth Rotation Effect

SATELLITE ORBIT INCLINATION = 80 DEGREES

LATITUDE OF BEACON = 30 DEGREES

TCA ELEVATION ANGLE = 60 DEGREES

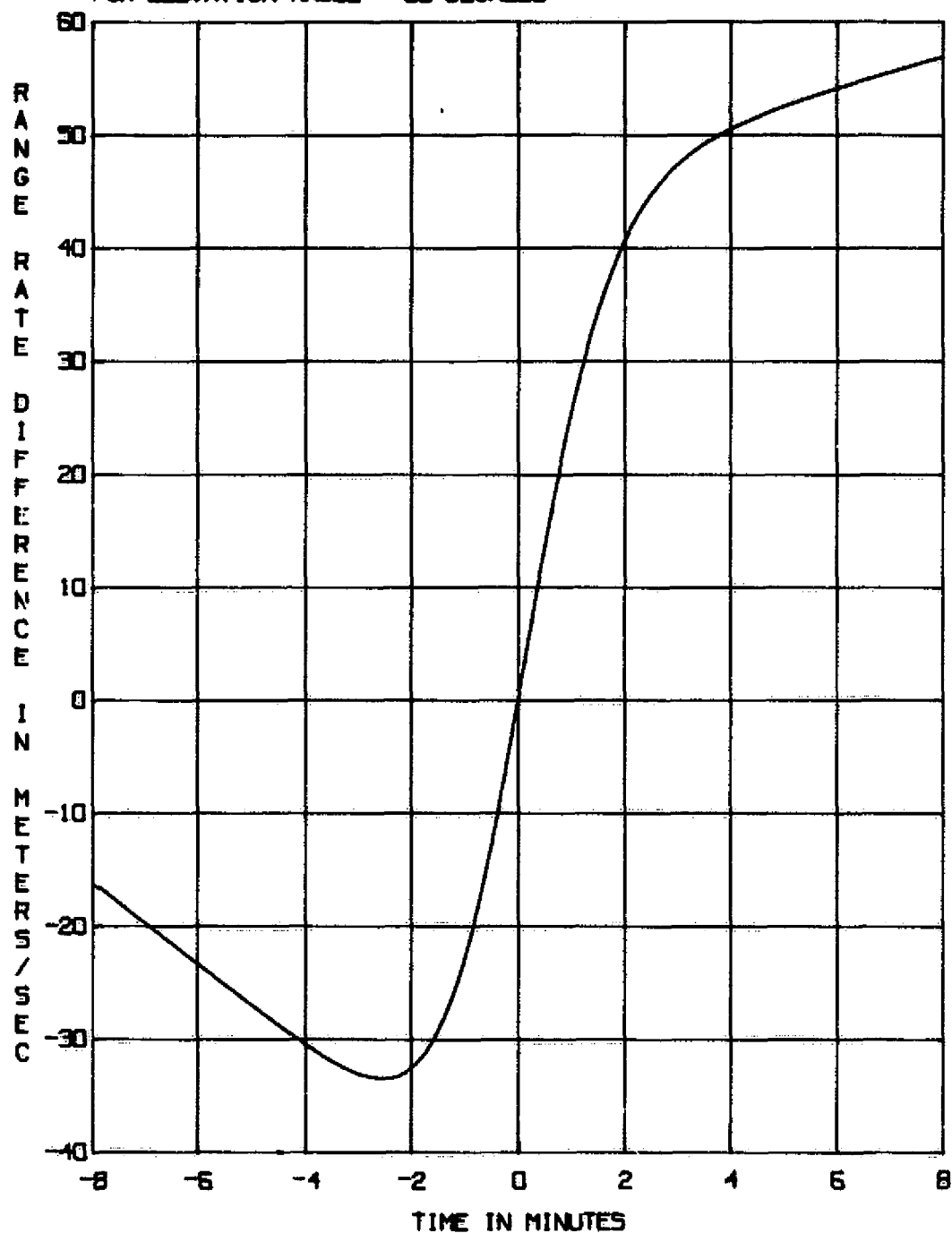


Figure 6. Earth Rotation Effect

SATELLITE ORBIT INCLINATION = 80 DEGREES

LATITUDE OF BEACON = 60 DEGREES

TCA ELEVATION ANGLE = 60 DEGREES

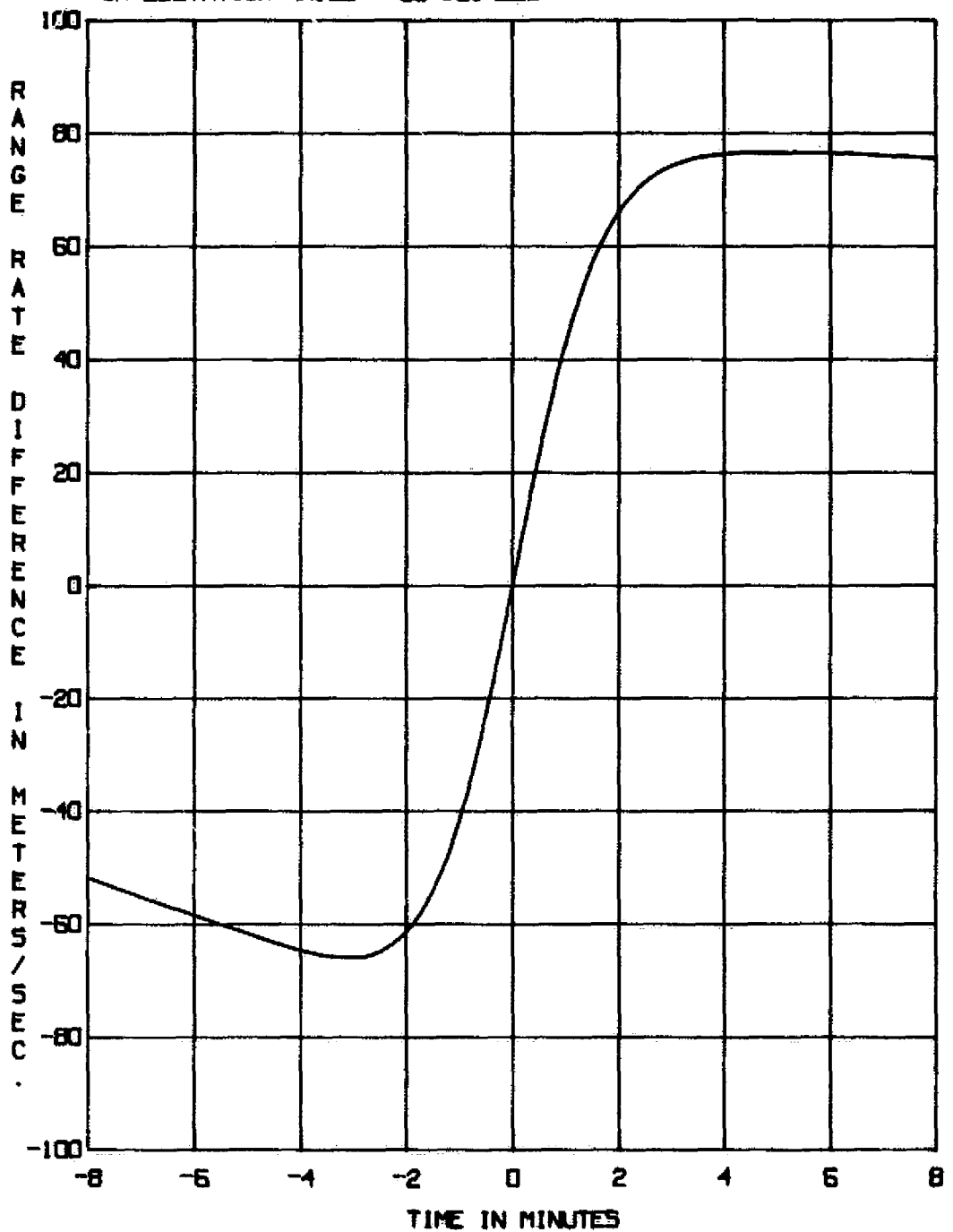


Figure 7. Earth Rotation Effect

### 3.3 Atmospheric Effects

As the signal from the beacon to the satellite traverses the Earth's atmosphere the Doppler frequency measurement will be altered. The atmosphere, for purposes of radiowave propagation, can be separated into two parts: the troposphere (sea level to 30 km) and the ionosphere (85 km to 1000 km). Troposphere refraction effects are generally frequency independent up to about 30 GHz. Ionospheric refraction is frequency dependent varying inversely as the square of the operating frequency. The atmospheric bias on Doppler results from a scanning by the ray path through media where the index of refraction is other than unity. This atmospheric bias is a function of index of refraction along the path, elevation angle and elevation angle rate.

#### TROPOSPHERE

If left uncorrected the maximum tropospheric induced range rate error is on the order of 10 cm/sec (0.13 Hz at 401.2 MHz) for a 1000 km altitude circular orbit satellite. This maximum effect will occur at low elevation angles for near overhead passes where elevation angle rates are highest. For systems such as the RAMS where RMS frequency noise is on the order of 0.5 Hz, this biasing effect is small in comparison. However even a rather simple algorithm can remove most of this tropospheric bias at elevation angles above 10° (Ref. 9). An estimate of range rate bias can be obtained using a series of well established approximations (Refs. 10, 11). In the troposphere the group and phase velocities are equal in magnitude and of the same sign. The range rate bias estimate can thus be obtained by differentiating the expression for range bias with respect to time. If an exponential atmosphere is assumed the resultant range rate bias estimates can be quickly derived. That is —

$$\Delta R_t = \frac{10^{-6}}{\sin E} \int_0^{30 \text{ KM}} N_s e^{-kh} dh = \frac{N_s 10^{-6}}{k \sin E} \quad (10)$$

Where:

$n_s = 1 + N_s (10^{-6})$  surface index of refraction

$N_s = 350$

$E$  = line-of-sight elevation angle beacon-to-satellite

$k$  = decay factor =  $1.6 \times 10^{-4}$  meters<sup>-1</sup>

and

$$\dot{\Delta R}_t = \frac{\partial \Delta R}{\partial t} = \frac{\partial \Delta R}{\partial E} \frac{\partial E}{\partial t} = - \left[ \frac{N_s (10^{-6}) \cos E}{k \sin^2 E} \right] \dot{E} \quad (11)$$

Now the elevation rate corresponding to an overhead circular pass can be written as:

$$\dot{E} = \frac{\pm \omega_s}{1 - \frac{1}{\left(1 + \frac{2ah + h^2}{a^2 \sin^2 E}\right)^{1/2}}} \quad (12)$$

where

$\dot{E}$  = elevation rate (positive sign for increasing elevation)

$h$  = satellite height = 1000 km

$a$  = earth radius = 6378 km

$\omega_s$  = satellite angular rate =  $10^{-3}$  radians/sec

For the values indicated the elevation angle rate is  $1.4 (10^{-3})$  radians/sec at  $10^\circ$  elevation and as previously stated using equation 11 the range rate bias is seen to be approximately -10 cm/sec. As the elevation angle approaches  $90^\circ$  (i.e. directly overhead) the troposphere range rate bias tends to zero.

## IONOSPHERE

A similar approximation can also be derived for the ionospheric Doppler effect (Ref. 12). For frequencies above about 100 MHz the index of refraction within the ionosphere can be expressed as:

$$n = \left( 1 - \frac{N_e e^2}{\epsilon_0 m \omega^2} \right)^{1/2} \approx \left( 1 - \frac{40.3 N_e}{f^2} \right) \quad (13)$$

where:

$N_e$  = Electron density (electrons/meter<sup>3</sup>)

$e$  = Electron charge =  $1.602 \times 10^{-19}$  coulombs

$m$  = Electron mass =  $9.11 \times 10^{-31}$  kilograms

$\epsilon_0$  = Free space dielectric constant

=  $8.855 \times 10^{-12}$  farads/meter

$\omega = 2\pi f$  (radians/sec)

It should be noted that within the ionosphere the index of refraction is less than unity and during a given satellite pass this results in a Doppler bias of opposite sign relative to tropospheric bias. The following expression includes a correction for horizontal gradient effects (e.g. day-to-night transitions) if information regarding the change in vertical electron content,  $I_v$ , is available in terms of the local elevation angle,  $E^*$ , at the height of electron density maximum,  $h_m$ .

$$\Delta \dot{R}_i = \left( \frac{40.3 I_v \cos E^*}{f^2 \sin^2 E^*} \right) \dot{E}^* \left( 1 - \overbrace{\frac{1}{I_v} \tan E^* \frac{dI_v}{dE^*}}^{\text{HORIZONTAL GRADIENT}} \right) \text{ meters/sec} \quad (14)$$

where:

$$I_v = \int_{85 \text{ KM}}^{1000 \text{ KM}} N_e \, dh \text{ (Electrons/meter}^2\text{)}$$

$f$  = frequency of transmission (Hz)

$E^*$  = local elevation angle of line-of-sight at height of maximum density

$\dot{E}^*$  = local elevation angle rate of line-of-sight at height of maximum density (radians/sec)

and from geometric considerations

$$E^* = \arccos \left[ \frac{a}{a + h_m} \cos E \right] \quad (15)$$

where:

$a$  = Earth radius (or spheroid radius of curvature if available — appendix A2.2)

$h_m$  = height of maximum electron density = 350 km

$E$  = elevation angle at beacon

$E^*$  = local elevation angle at  $h_m$

$$\dot{E}^* = \left\{ \frac{a \dot{E} \sin E}{a + h_m} \right\} \left\{ \frac{1}{\left[ 1 - \left( \frac{a}{a + h_m} \right)^2 \cos^2 E \right]^{1/2}} \right\} \quad (16)$$

where:

$\dot{E}$  = elevation angle rate as observed at beacon

$\dot{E}^*$  = elevation angle rate at  $h_m$

The vertical integrated electron content can vary between  $10^{16}$  and  $10^{18}$  electrons/meter<sup>2</sup> depending on geographical location, season, time of day, sun spot cycle and so on. The continuously updated NASA world ionospheric model developed for providing ionospheric corrections to NASA tracking data is one source of integrated content values for offline corrections to beacon data. The expression given by equation 14 can be used to provide estimates of maximum ionospheric effects. For purposes of comparison with tropospheric effects a ground elevation,  $E$ , of  $10^\circ$  is again assumed along with a ground elevation rate,  $\dot{E}$ , of  $1.40 \times 10^{-3}$  radians/sec. A typical daytime vertical integrated content of  $3 \times 10^{17}$  electrons/meter<sup>2</sup> with no horizontal gradient is also assumed. Using the foregoing, this results in a maximum 401.2 MHz range-rate bias of 35 cm/sec (Doppler bias -0.5 Hz). At 100 MHz this bias increases to 6 meters/sec (Doppler bias -2 Hz).

Since system frequency measurement resolution will typically be 1 Hz or better, an ionospheric correction in the 100 MHz region is imperative. At 400 MHz and above, such a correction is optional but should be included if full system capability is to be realized. While the atmospheric effect has been referred to as a bias, it actually has a time varying characteristic over the full satellite pass. It therefore cannot be as easily solved for as, for example, the oscillator frequency offset which is nearly constant over the satellite pass.

Using beacon frequencies higher than 400 MHz will further reduce ionospheric Doppler effects. However, if simple low gain (and hence broadbeam) antennas are used at both satellite and beacon to optimize coverage (Ref. 13), a nominal link frequency of 400 MHz is probably a good choice.

### 3.4 Orbit Update Procedure

Accurate recovery of the unknown beacon's coordinates is directly dependent on the accuracy of the reference orbit. In practice it is found that the absolute accuracy of the reference orbit deteriorates with time resulting in a corresponding degradation in the accuracy of the recovered beacon coordinates. The most significant error in the reference orbit is the one associated with the "along track" error. This error may be thought of as an error in the mean anomaly or alternatively, as an error in the epoch time of the reference orbit. Using Doppler data from a beacon of known position the orbit update procedure solves for this "along track" error and corrects the reference orbits epoch time accordingly. Each range rate (Doppler) observation is considered to be a function of the reference orbit's epoch time  $T$ , and the range rate bias  $B$ . The linearized observational equation is then given by,

$$\dot{R}^o - \dot{R} = \frac{\partial \dot{R}}{\partial T} \Delta T + \Delta B \quad (17)$$

where,

$\dot{R}^o$  = observed range rate

$\dot{R}$  = "computed" range rate — based on reference epoch  $T$ , and beacon position

$\frac{\partial \dot{R}}{\partial T}$  = partial derivative of "computed" range rate with respect to epoch time  $T$ .

$\Delta T$  = correction to epoch time  $T$

$\Delta B$  = correction to range rate bias

As a practical matter the partial derivative is computed numerically as a first difference, — that is,

$$\frac{\partial \dot{\mathbf{R}}}{\partial \mathbf{T}} = \frac{\dot{\mathbf{R}}(\mathbf{T} + \Delta \mathbf{T}) - \dot{\mathbf{R}}(\mathbf{T})}{\Delta \mathbf{T}} \quad (18)$$

Experience has shown that for the geometries considered in this paper, a value of  $\Delta \mathbf{T}$  equal to one second is a satisfactory interval when using the approximations indicated by equations 17 and 18. The quantities  $\Delta \mathbf{T}$  and  $\Delta \mathbf{B}$  are then solved for using the method of least squares. Each data point is processed for inclusion in a set of normal equations designed to yield the updated orbit solution. Let  $\mathbf{N}$  represent the 2 by 2 normal matrix with elements  $N_{ij}$ . The four matrix elements are evaluated (e.g. Ref. 24) as follows:

$$\begin{aligned} N_{11} &= \sum_{m=1}^n \left( \frac{\partial \dot{\mathbf{R}}}{\partial \mathbf{T}_m} \right)^2 \\ N_{12} &= N_{21} = \sum_{m=1}^n \left( \frac{\partial \dot{\mathbf{R}}}{\partial \mathbf{T}_m} \right) \\ N_{22} &= \text{number of data points} = n \end{aligned} \quad (19)$$

and,

$$\mathbf{N} = \begin{bmatrix} N_{11} & N_{12} \\ N_{21} & N_{22} \end{bmatrix}$$

similarly the 2 by 1 matrix

$$\mathbf{C} = [c_1 \ c_2]^T$$

is evaluated as:

$$c_1 = \sum_{m=1}^n (\dot{\mathbf{R}}^o - \dot{\mathbf{R}})_m \frac{\partial \dot{\mathbf{R}}}{\partial \mathbf{T}_m} \quad c_2 = \sum_{m=1}^n (\dot{\mathbf{R}}^o - \dot{\mathbf{R}})_m \quad (20)$$

Again all sums are carried over all n data points since a separate linearized equation exists at each measurement time.

The least squares solution is obtained by solving this normal system of linear equations and is given by,

$$\begin{bmatrix} \Delta \mathbf{T} \\ \Delta \mathbf{B} \end{bmatrix} = \mathbf{N}^{-1} \mathbf{C}$$

and finally,  $\mathbf{T} = \mathbf{T}_0 + \Delta \mathbf{T}$  and  $\mathbf{B} = \mathbf{B}_0 + \Delta \mathbf{B}$  represent the current solution values ( $\mathbf{T}_0$  and  $\mathbf{B}_0$  being initial values) which are used as starting values for the next iteration. This iterative process is considered to have converged when the absolute value of the  $\Delta \mathbf{T}$  and  $\Delta \mathbf{B}$  corrections are acceptably small.

This newly solved for value of orbit epoch time  $\mathbf{T}$ , is then used to update the reference orbit on all subsequent solutions for unknown beacon locations. A definite improvement in the recovery of beacon coordinates results if this procedure is used on each orbital pass. This requires that at least one reference beacon be available on each pass. The procedure itself is automatic, the only information needed is the identification number of the surveyed in reference beacon which as a matter of convenience can be located at the site receiving the satellite relayed Doppler data.

### 3.5 Error Sources

The accuracy of beacon position location computations will be influenced by Doppler data quality and quantity; beacon-to-satellite geometry; and accuracy of satellite ephemeris. Means for upgrading the satellite ephemeris were discussed in the previous section. Except for the near overhead pass case, satellite position errors couple approximately into equivalent beacon position errors. That is if the orbit is well determined (known within tens of meters) the contribution to position location error will be in the tens of meters. Error studies (e.g. Ref. 14) indicate, however, for the near overhead case position location errors become as large as ten times the satellite position error.

Doppler data processing experience has shown that for the single pass case, beacon height above the geoid is generally not observable. It can be shown that this error translates into a position error approximately equal to the height uncertainty multiplied by  $\tan E$ , where  $E$  is the beacon-to-satellite elevation angle. If more than one pass of data is available from a stationary beacon, height can be solved for along with latitude, longitude and frequency bias. The minimum number of data points required for a position determination will of course equal the number of unknowns being solved for.

The data quality is governed by such factors as time tag accuracy and frequency stability throughout the system. Time tag errors couple indirectly and are indistinguishable from along track orbit errors. For example, a 0.1 second time error is equivalent in effect to an 700 meter along track error

since the spacecraft velocity is approximately 7 km/sec. The NIMBUS-6 TWERLE/RAMS system was designed for a  $\pm 5$  km single pass position accuracy and hence a time tag accuracy of  $\pm 0.1$  seconds was adequate. The TIROS-N time tag for an equivalent Doppler tracking system will be  $\pm 0.010$  seconds.

Another important factor is the overall frequency stability including beacon transmitter and all heterodyning oscillators up through the average frequency measurement. Generally the RAMS system provides sufficient data (e.g. 10 or more Doppler points at a one per minute rate) such that the noise (typically 0.5 Hz at 401.2 MHz) and the solved for bias offset (typically several KHz) are of little or no consequence in terms of location accuracy. The noise is averaged by the least squares fitting technique and the bias is easily extracted to within system resolution values ( $\pm 1$  Hz). However long term oscillator drift, which changes the slope of the Doppler curve, will introduce position errors. Both simulations and error analyses indicate that the RAMS sensitivity to frequency drift for a full Doppler data span can be estimated by a simple expression deduced from an approximate differentiation of equation (7) namely:

$$\Delta S \approx \left( \frac{V}{R} \right)^2 \left( \frac{\dot{f}}{f_T} \right) \left( \frac{c}{\cos E} \right) = \frac{c \dot{f} (10^5)}{f_T \cos E} \text{ meters} \quad (21)$$

where:

$\Delta S = \frac{\Delta R}{\cos E}$  position error (meters)

$\Delta R$  = beacon-to-satellite error (meters)

$c$  = speed of light (meters/sec)

$f_T$  = beacon nominal frequency (Hz)

$\dot{f}$  = frequency drift (Hz/sec)

$E$  = beacon-to-satellite elevation

$V$  = satellite speed =  $7.35 \times 10^3$  meters/sec

$\ddot{R}$  = typical maximum acceleration = 25 meters/sec<sup>2</sup>

By observing changes in frequency bias on consecutive passes,  $\Delta f$  has been observed to be typically 1 Hz per 1000 seconds for the RAMS system. The expected position error corresponding to such a drift at 401.2 MHz for a TCA elevation of 45° will therefore be on the order of 100 meters. At a TCA elevation of 80° this error would increase to 400 meters.

The effect of the atmosphere is to change the slope of the Doppler curve and in this sense introduces an error in position location very similar to that due to frequency drift. For example, as indicated in the previous section, an ionospheric excursion of  $\pm 2$  Hz at 100 MHz can easily be expected for a near overhead pass. If this change occurs over a typical 1000 second pass an "equivalent drift" of 0.004 Hz/sec is experienced. Putting this value into equation 21 and assuming a TCA elevation of 80° indicates an expected position error of 6 km. At 401.2 MHz this effect for an uncorrected daytime ionosphere ("equivalent drift" of 0.001 Hz/sec) and the same geometry would be on the order of 0.4 km. If even a nominal correction is made based upon equation 14 this error can be reduced to 30% of the uncorrected value. A two frequency scheme such as associated with the Navy Transit system can be employed to provide real-time ionospheric corrections which even during high solar activity reduce this error to a value on the order of 10 meters (Ref. 15). If only a portion of the Doppler curve is used for position determination the error due to frequency drift is reduced. However in this case the position error due to data noise increases to the extent that frequency noise often becomes the predominant system error source.

#### 4.0 MICROCOMPUTER DESCRIPTION

Ever since the 1975 NIMBUS-6 launch, the computations required for position location of buoys, meteorological balloons, and other experimental platforms using the NIMBUS-6 RAMS system have been successfully carried out using a centrally located conventional general purpose computer. Doppler position location systems similar to the NIMBUS-6 scheme will be carried by one or more of the forthcoming series of TIROS-N spacecraft. The TIROS-N platform monitoring and position location system will be applied to both user community platforms and "distress beacon" locations during the Satellite Aided Search and Rescue Demonstration. Much interest has been expressed by the NASA user community in being able to set up low cost terminals capable of receiving and processing NIMBUS-6 and TIROS-N telemetry and Doppler data directly at the user's site. It is in direct response to this user need that the prototype micro-computer described in this paper was developed. The required low cost, compact, and reliable computer facility suitable for a self contained user terminal has been made possible through the advent of large-scale integration (LSI) microelectronic circuits (Ref. 16) where thousands of circuit elements are integrated in one chip. For example typical Random-Access Memory (RAM) chips measuring 3 by 5 millimeters provide an equivalent of over 16,000 transistors where each "transistor cell" is capable of storing one binary bit of information (Ref. 17).

In such chips the time required to write one bit in an arbitrary location or to read it out is about 200 nanoseconds. The remainder of this section will discuss how such LSI chips were interconnected and programmed to perform the specific task of computing beacon latitude and longitude using

satellite observed Doppler frequency data and the known satellite orbit as input. Microcomputer alphanumeric output has been obtained using either a standard teletype printer or a cathode ray tube readout. The microcomputer input has been successfully interfaced and accepted data in a variety of ways including: paper tape via the teletype terminal; teletype keyboard; American Standard Code for Information Interchange (ASCII) keyboard for direct manual entry; cassette tape recorder output; and direct real time tie in to a NIMBUS-6 telemetry receiver. The next few sections will discuss the Central Processing Unit, Memory, and Input-Output Peripherals of the NIMBUS-6/TIROS-N position location microcomputer. The total power requirement for this microcomputer is on the order of 7 watts (+5 V at 1.2 A and +12 V at 0.1 A).

The basic block diagram of the microcomputer and interface is shown in Figure 8.

#### 4.1 Central Processing Unit

Every computer requires some type of central processing unit (CPU) where the actual computing is carried out. The CPU usually controls all the operations of the computer. Computers designed as recently as ten years ago used CPUs consisting of rows of printed circuit boards requiring a fairly large enclosure to house all CPU related components. Today the entire CPU can reside on a single LSI microprocessor chip (Ref. 18). At present there are over 50 different microprocessor chips on the market (Ref. 19). In the position location microcomputer the particular LSI chip incorporated is the 40 pin MOS Technology, Inc. type MCS 6502 which incorporates an 8 bit data bus (Ref. 20). This chip provides a 16 pin address bus and therefore is capable of addressing up to  $2^{16}$  or 65,536 bytes of memory where a byte by definition consists of 8 bits. The

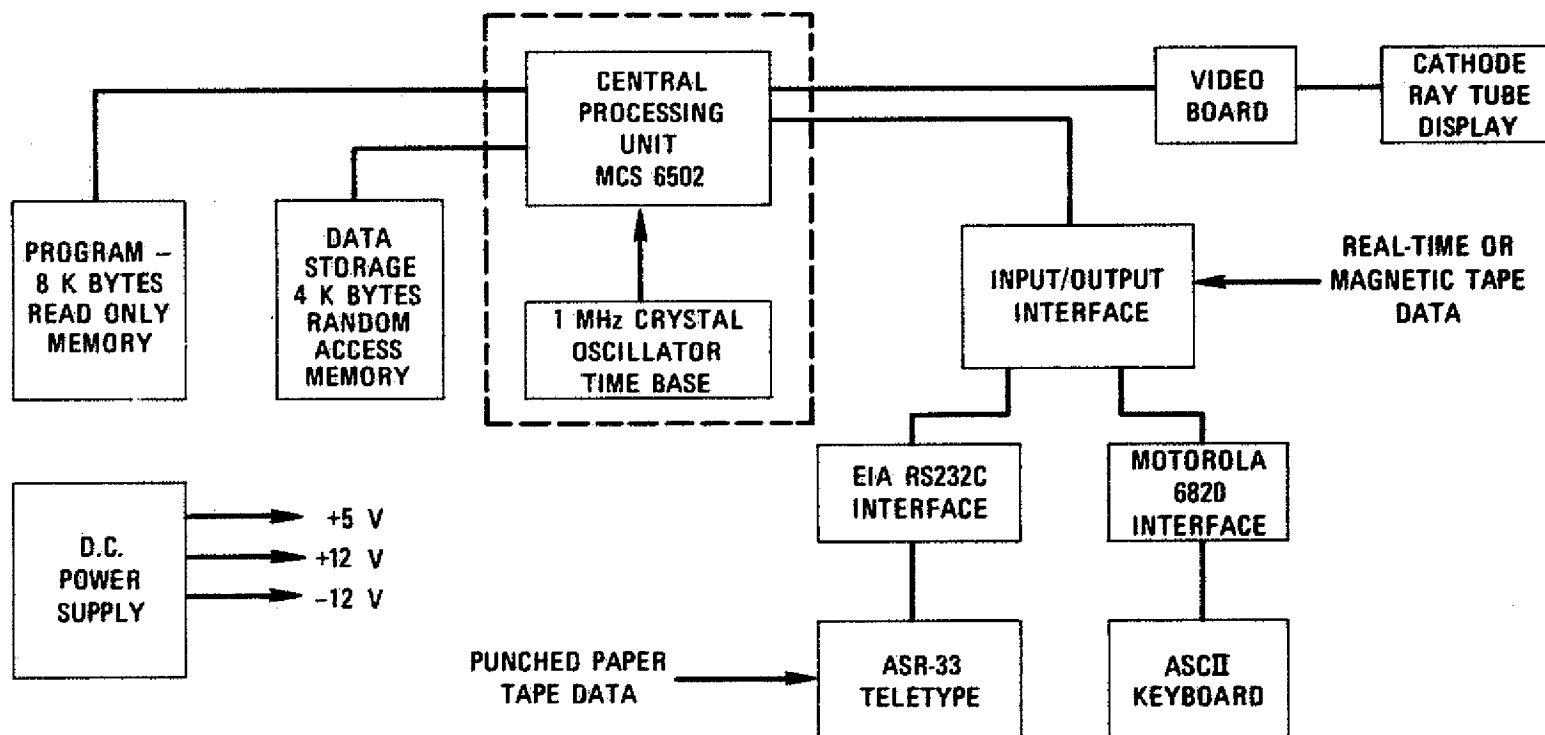


Figure 8. Basic Position Location Microcomputer and Interface

term "bit" refers to anything that can be assigned a binary value of 0 or 1. The MCS6502 has the basic timing oscillator and clock driver on chip, thus eliminating the need for an external high level two-phase clock generator. This CPU chip can be used with an externally generated time base consisting of either a transistor-transistor logic (TTL) level single-phase clock, crystal oscillator, or RC network. In this application an external time base consisting of a 1 MHz crystal oscillator is used to generate the required two phase clock pulses. Nominal clock pulse width is 430 nsec. As in most microcomputer systems, the timing of all data transfers is controlled by the system clock. The clock itself is actually two non-overlapping square waves. This "two-phase" clock system essentially provides two consecutive positive going switching pulses where the address lines and read-write commands are set up during the first pulse and data is transferred (either read or write) during the second pulse.

There are also two interrupt input lines to the microprocessor. The primary purpose of these lines is to permit a mode of operation which minimizes the computer time spent in interrogating input peripheral devices and reading out via output peripheral devices except during times of specific interest.

The internal organization of the processor can be split into two sections. In general, the instructions obtained from program memory are executed by implementing a series of data transfers in the "register section" of the chip. The control lines which actually cause the data transfers to take place are generated in the "control section".

Instructions enter the processor on the data bus, are latched into the instruction register, and are then decoded along with timing signals to generate the register control signals.

The timing control unit keeps track of the specific cycle being executed.

Each data transfer which takes place in the register section is caused by decoding the contents of both the instruction register and the timing counter. Additional control lines which affect the execution of the instructions are derived from the Interrupt logic and from the Processor Status register. The Interrupt logic controls the processor interface to the interrupt inputs to assure proper timing, enabling, sequencing, etc. which the processor recognizes and services.

The Processor Status register contains a set of latches which serve to control certain aspects of the processor operation, to indicate the results of processor arithmetic and logic operations, and to indicate the status of data either generated by the processor or transferred into the processor from outside.

The real work in the microprocessor is carried out in the register section of the chip. At 1 MHz, the data coming into the processor from the program memory, the data memory, or from peripheral devices, appears on the data bus during the last 100 nanoseconds of the second (or phase two) positive clock pulse. No attempt is made to actually operate on the data during this short period. Instead, it is simply transferred into the input data latch for use during the next cycle. The data latch serves to trap the data on the data bus during each Phase Two pulse. It can then be transferred onto one of the internal busses and from there into one of the internal registers. For example, data being transferred from memory into the "accumulator" will be placed on the internal data bus and will then be transferred from the internal data bus into the accumulator. If an arithmetic or logic operation is to be performed using the data from memory and the contents of the accumulator, data in the input data latch will be transferred onto the internal data bus as before. From there it will be transferred

into the "arithmetic logic unit" (ALU). At the same time the contents of the accumulator will be transferred onto a bus in the register section and from there into the second input to the ALU. The results of the arithmetic or logic operation will be transferred back to the accumulator on the next cycle by transferring first onto the bus and then into the accumulator. All of these data transfers take place during the Phase One clock pulse. There is also a "program counter" which provides the addresses which sequentially step the processor through instructions in the program which resides in memory.

The accumulator is a general purpose 8-bit register which sorts the results of most arithmetic and logic operations. In addition, the accumulator usually contains one of the two data words used in these operations.

All logic and arithmetic operations take place in the ALU. However, the ALU cannot store data for more than one cycle. If data is placed on the inputs to the ALU at the beginning of one cycle, the result is always gated into one of the storage registers or to external memory during the next cycle. Each bit of the ALU has two inputs. These inputs can be tied to various internal busses or to a logic zero; the ALU then generates the SUM, AND, OR, etc. function using the data on the two inputs. The "stack pointer" and the two "index registers" each consist of 8 simple latches. These registers store data which is to be used in calculating addresses in data memory. The address bus buffers consist of a set of latches and TTL compatible drivers. These latches store the addresses which are used in accessing the peripheral devices (ROM, RAM, and INPUT/OUTPUT).

The microprocessor accesses position of memory for program instructions and  $\epsilon$  to perform the overall computer function.

## 4.2 Data and Program Memory

### DATA

The memory section of the microcomputer is in two distinct segments. The data which consists of the Doppler measurements performed by the satellite as it passed over the radio beacon is stored in 4 k bytes of Random Access Memory (RAM). The term "random access" means that any word in the memory may be accessed without having to go through all the other words to get to it. The only drawback of RAM memory is that when power is lost from the chip all memory content is lost.

The Doppler data is loaded into the computer in any of a number of ways including: punched paper tape via the teletype, magnetic tape, real time NIMBUS-6 receiver tie in or manual entry via the keyboard. Also stored in this memory bank are the coordinates and velocity of the satellite at some epoch time near the time of data collection. As indicated in section 3.4 the microcomputer has the capability of refining this orbit if Doppler data from one or more reference beacons is available. The satellite position and velocity over the Doppler pass are computed at the time of each data point and the memory need only store the 6 numbers representing the satellite state vector at one point in time. In addition to this "data storage" the RAM also provides a certain amount of "working storage". This is required for such things as storage of intermediate results in arithmetic operations and peripheral output data storage. The RAM of the position location microcomputer discussed in this paper consists of 32 type 2102 RAM chips, where each chip has 1024 bits of memory.

## PROGRAM

Program algorithms are those discussed in the body of the paper and the appendix. Originally as the position location least squares program evolved, it was loaded into RAM using a cassette type magnetic tape. After the program design was achieved it was loaded into Read Only Memory (ROM) chips or more correctly into an Erasable Programmable Read Only Memory (EPROM). These particular chips are permanently programmed by means of a "PROM Programmer Unit". The memory can only be erased after a several minute exposure under a special high intensity ultraviolet light. Once erased, the chips can be reprogrammed. This particular program memory consists of eight type 2708 EPROMs where each EPROM chip contains 1024 bytes of storage for a total program storage of 8192 bytes.

It should be mentioned that a complete floating point math pack of subroutines is included in the EPROM to allow evaluations of all arithmetic algorithms including multiplication, division, trigonometric and exponential functions. The overall floating point microcomputer precision is 12 decimal digits which is more than adequate for this particular application.

### 4.3 Input-Output Peripherals

As already suggested a wide variety of peripherals can be interfaced with the microcomputer. Figure 9 shows the microcomputer interfaced with a keyboard and CRT video display. Figure 10 shows a close up of the printed circuit

ORIGINAL PAGE IS  
OF POOR QUALITY

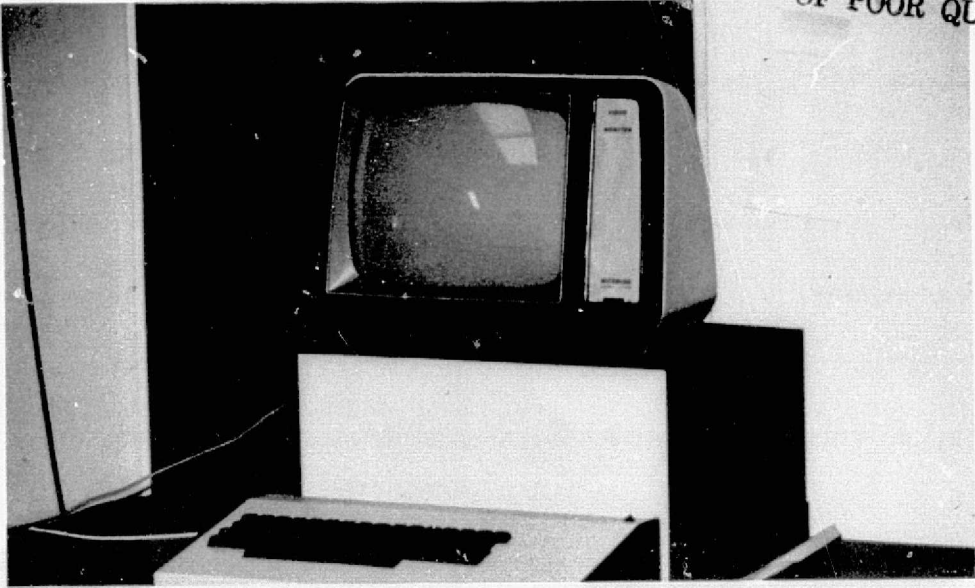


Figure 9. Position Location Microcomputer

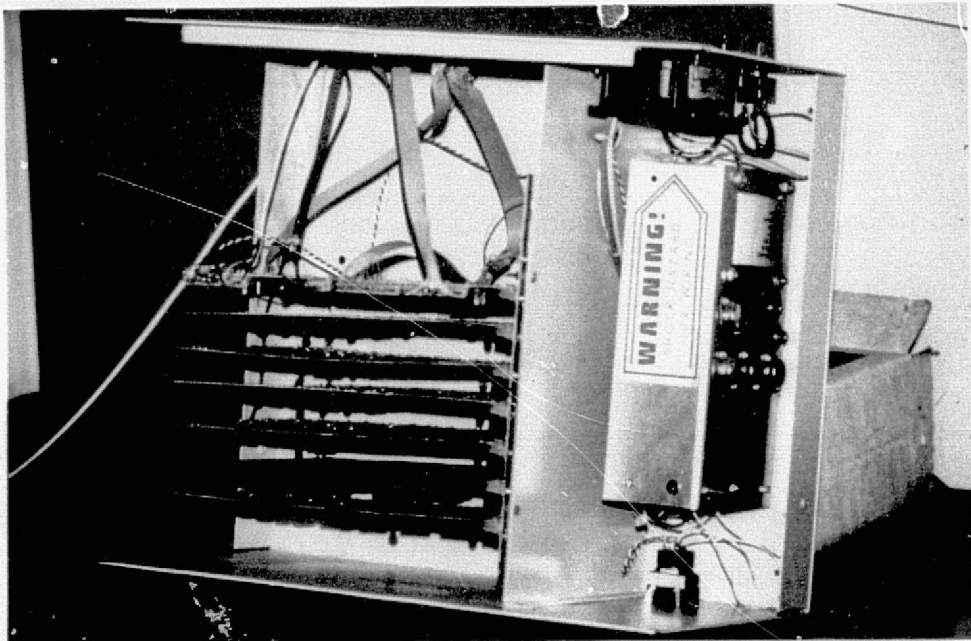


Figure 10. Microcomputer Printed Circuit Cards

cards which make up the microcomputer along with the required d.c. power supply. One important consequence of this position location microcomputer development is a demonstration of the relative ease with which such a computer can be interfaced with the "outside world". The controlled transfer of data and program information between the processor and numerous peripheral devices (i.e. "handshaking") has been carried out. In fact, a Cross Assembler was used where output from a DEC PDP 11-40 directly programmed the EPROM in the microcomputer. Whenever changes were to be evaluated, a new EPROM was plugged in and programmed. When the program was considered obsolete the EPROM was erased using ultraviolet light and hence made ready for future programming. Of course, certain portions of the programming such as the "math pack", once checked out required no further modification. The computation time for a typical Doppler pass of 15 data points over a 10 minute observation interval is typically 20 seconds per least squares iteration. Usually 3 iterations are sufficient to provide a converged or final solution. The computer recognizes the platform identification I-D (as contained in the telemetry) of each platform and sequentially stores the data in RAM as it comes. As many as 50 platforms may be tracked at any given time by NIMBUS-6. Once the data is collected the operator "punches up" the I-D of those platforms he is interested in computing positions for. The microcomputer then scans the data portion of the RAM for one particular I-D and at each data time computes the satellite position and velocity as well as the partial derivatives required for the least squares solution (see appendix). Once all the partials and satellite vectors have been computed for a given beacon the solution is obtained and printed out in alphanumeric either on teletype or CRT. Then the computer goes on to the

next I-D and so on. Experience has shown that given the same Doppler data set and orbit information the microcomputer computes the same (to 8 significant figures) position as much larger general purpose machines such as the IBM 360-95 or the DEC PDP11-40. Finally, if the input data is stored on punched paper tape, an optical reader has been shown to be an ideal low cost way to rapidly read in information to the microcomputer RAM. In this mode the data is read in as fast as the tape moves under an illuminating lamp.

## 5.0 NIMBUS-6 RESULTS

Numerous RAMS type beacon location computations have been performed using the position location microcomputer. Also along track corrections to the nominal NIMBUS-6 orbit have been made using the reference 401.2 MHz beacon located at GSFC, Greenbelt, Maryland. The NIMBUS-6 spacecraft is tracked by the NASA Minitrack interferometer tracking network. The "definitive orbits" using this angle tracking data are provided about two weeks after the data is taken and are accurate to better than a few hundred meters. Long term (one month or more ) orbit predictions for antenna pointing and data acquisition purposes will be significantly less accurate. In either case real time orbit improvements can be realized using one or more reference beacons. In fact, if several such reference beacons are deployed, a real time geometric solution can be made and the need for orbit data is obviated.

Figure 11 presents some typical beacon location results using the NIMBUS-6 RAMS system and position location microcomputer. These particular passes were handled in real time — that is, as soon as the data was recorded the position location computations were performed. It has been observed that the

PLATFORM I-D	NIMBUS-6 ORBIT NUMBER	BEACON GEOGRAPHICAL AREA	SINGLE PASS POSITION LOCATION (DEGREES)		DIFFERENCE FROM REFERENCE (DEGREES)		RMS DATA NOISE (Hz)
			LATITUDE	LONGITUDE	$\Delta$ LAT.	$\Delta$ LONG.	
171	7863	GULF OF MEXICO	26.014	-93.475	0.004	0.015	1.3
722	7863	GULF OF MEXICO	30.090	-88.847	0.003	0.001	1.3
117	7864	GREENBELT, MARYLAND	39.005	-76.823	0.005	0.003	1.5

Figure 11. Typical Position Location Results

Doppler data noise as determined from the RMS residuals of observed minus computed Doppler (see appendix) is typically less than 2 Hz at 401.2 MHz. This is consistent with the RAMS frequency resolution of  $\pm 1$  Hz corresponding to a range-rate resolution of  $\pm 1.3$  meters/sec.

## 6.0 CONCLUSIONS

A low cost, accurate and reliable special purpose microcomputer for the real time computation of position locations of radio beacons observed by satellite has been successfully developed and tested. This basic microcomputer design will be incorporated in two NASA NIMBUS-6/TIROS-N low cost Local User Terminals (LUT) currently being assembled for demonstration purposes. The LUT will be totally automatic with the azimuth-elevation antenna drive information also provided by the microcomputer. The position location of beacons will automatically be provided on a single pass and two consecutive pass basis. This allows for improved accuracy of fixed beacons and position change computation of drifting beacons (i.e. buoys). The position computation accuracy is dependent on orbit accuracy and Doppler data quality under various geometries. The microcomputer computational accuracy is consistent with that obtained with much larger general purpose computers to 8 decimal digits in floating point arithmetic.

## APPENDIX

### LEAST-SQUARE MICROCOMPUTER ALGORITHM

The following relationships are programmed along with the "math package" in sectors of the microcomputer EPROM and are called up as required. The particular mathematical relation called up will depend on the type input being provided. For example if the satellite orbit information is already given in geocentric Earth fixed coordinates the Earth rotation matrix computation will not be used and so on. The desired beacon position is always in Earth fixed coordinates (i.e. latitude and longitude) and once the satellite position and velocity are expressed in Earth fixed coordinates the time varying range rate (Doppler) between beacon and satellite is easily expressed (e.g. equation 2). Conventional coordinate transformations (Ref. 21) are incorporated in the microcomputer. A least squares (Refs. 22, 23, 24) technique is applied in the data reduction to assure maximum position location accuracy.

## A.1 COORDINATE SYSTEMS

### A.1.1 Geocentric Inertial of Date (Cartesian)

This system has its origin at the center of the Earth. The  $u$  and  $v$  axes lie in the equatorial plane with the  $u$  axis towards the vernal equinox of date. The  $w$  axis is positive through the north pole, and the  $v$  axis in a direction such that a right handed coordinate system is formed.

### A.1.2 Geocentric Earth Fixed (Cartesian)

The origin of this system is also at the center of the Earth. As in the Geocentric Inertial system the  $x$  and  $y$  axes lie in the equatorial plane however the  $x$  axis passes through the Greenwich meridian. The positive  $z$  direction is again directed towards the north pole and the direction of the  $y$  axis is consistent with a right handed coordinate system.

## A.2 COORDINATE TRANSFORMATIONS

### A.2.1 Geocentric Inertial to Geocentric Earth Fixed

The transformation is given by:

$$\begin{bmatrix} x \\ y \\ z \end{bmatrix} = A(\vartheta) \begin{bmatrix} u \\ v \\ w \end{bmatrix} \quad \text{A-1}$$

Where  $\vartheta$  is the angle between the line formed from the center of the Earth to the true vernal equinox and the Geocentric Earth fixed  $x$  axis.

$\vartheta$  is usually available as:

$$\vartheta = \vartheta_0(t_0) + \dot{\vartheta}(t - t_0)$$

and  $\vartheta_0$  is the angle at

$t_0 = 0$  hours GMT of the epoch day and

$t$  = epoch time GMT

$\dot{\vartheta}$  = Earth rotation rate

The Earth fixed velocities are given by:

$$\begin{bmatrix} \dot{x} \\ \dot{y} \\ \dot{z} \end{bmatrix} = A(\vartheta) \begin{bmatrix} \dot{u} \\ \dot{v} \\ \dot{w} \end{bmatrix} + \dot{A}(\vartheta) \begin{bmatrix} u \\ v \\ w \end{bmatrix} \quad \text{A-2}$$

in all of the above:

$$A(\vartheta) = \begin{bmatrix} \cos \vartheta & \sin \vartheta & 0 \\ -\sin \vartheta & \cos \vartheta & 0 \\ 0 & 0 & 1 \end{bmatrix} \quad \text{A-3}$$

$$\dot{A}(\vartheta) = -\dot{\vartheta} \begin{bmatrix} \sin \vartheta & -\cos \vartheta & 0 \\ \cos \vartheta & \sin \vartheta & 0 \\ 0 & 0 & 0 \end{bmatrix} \quad \text{A-4}$$

### A.2.2 Geodetic Latitude and Longitude to Geocentric Earth Fixed

The Earth shape and beacon location parameters are as follows:

$a$  = equatorial radius of Earth reference spheroid

$e$  = reference spheroid eccentricity

$\varphi$  = geodetic latitude of beacon (positive north)

$\lambda$  = longitude of beacon (positive east)

$h$  = height of beacon above reference spheroid

Let  $r$  represent the magnitude of the radius of curvature in the plane of the prime vertical then:

$$r = \frac{a}{(1 - e^2 \sin^2 \varphi)^{1/2}}$$

and the beacon's geocentric coordinates are given by:

$$S_1 = (r + h) \cos \varphi \cos \lambda$$

$$S_2 = (r + h) \cos \varphi \sin \lambda \quad \text{A-5}$$

$$S_3 = [r(1 - e^2) + h] \sin \varphi$$

### A.2.3 Geocentric Earth fixed to Local Elevation

The atmospheric corrections (section 3.3) require computation of local elevation,  $E$ , and local elevation angle rate,  $\dot{E}$ .  $E$  and  $\dot{E}$  are obtained as follows: for the local topocentric Earth fixed cartesian coordinate system  $\ell_1, \ell_2, \ell_3$ ;

$$E = \tan^{-1} \ell_3 (\ell_1^2 + \ell_2^2)^{-1/2} \quad \text{A-6}$$

$$\dot{E} = \frac{\partial E}{\partial \ell_1} \dot{\ell}_1 + \frac{\partial E}{\partial \ell_2} \dot{\ell}_2 + \frac{\partial E}{\partial \ell_3} \dot{\ell}_3 \quad \text{A-7}$$

$$\begin{bmatrix} \ell_1 \\ \ell_2 \\ \ell_3 \end{bmatrix} = M \begin{bmatrix} x - S_1 \\ y - S_2 \\ z - S_3 \end{bmatrix} \quad \text{A-8}$$

where  $x, y, z$  and  $S_1, S_2, S_3$ , are Geocentric Earth fixed coordinates corresponding to the satellite and beacon respectively. And the rotation matrix  $M$  is given by:

$$M = \begin{bmatrix} -\sin \lambda & \cos \lambda & 0 \\ -\sin \phi \cos \lambda & -\sin \phi \sin \lambda & \cos \phi \\ \cos \phi \cos \lambda & \cos \phi \sin \lambda & \sin \phi \end{bmatrix} \quad \text{A-9}$$

also since the beacon is Earth fixed:

$$\begin{bmatrix} \dot{\ell}_1 \\ \dot{\ell}_2 \\ \dot{\ell}_3 \end{bmatrix} = M \begin{bmatrix} \dot{x} \\ \dot{y} \\ \dot{z} \end{bmatrix} \quad \text{A-10}$$

which permits  $\dot{E}$  to be computed as:

$$\dot{E} = \frac{(\ell_1^2 + \ell_2^2) \dot{\ell}_3 - \ell_3 (\ell_1 \dot{\ell}_1 + \ell_2 \dot{\ell}_2)}{R^2 (\ell_1^2 + \ell_2^2)^{1/2}} \quad \text{A-11}$$

where the slant range,  $R$ , is computed from

$$R^2 = (x - S_1)^2 + (y - S_2)^2 + (z - S_3)^2 \quad \text{A-12}$$

The atmospheric corrections are not applied until after the first least squares

iterative beacon solution for  $S_1, S_2, S_3$ , (or equivalently  $\phi, \lambda$ ) to assure proper convergence.

### A.3 LINEAR LEAST SQUARES SOLUTION FOR BEACON LONGITUDE AND GEODETIC LATITUDE

The least squares approach incorporated in the microcomputer is conventional in that the equation of observation (equation 2 of text plus a constant bias term) is linearized. The result is a set of linear equations equal to the number of Doppler data points. In general the number of points (hence, equations) will exceed the number of unknowns which in this case is three (latitude, longitude and range rate bias). The procedure outlined in the following indicates how this set of linear equations are reduced to a new set, namely; the normal equations, where the number of equations equals the number of unknowns. The solution of the normal equations in the microcomputer is achieved in a predetermined number of iterations (usually 3). The resultant least squares solution is considered to have converged when successive iterations alter the result by an amount less than that attributable to data noise.

By expanding the equation of observations in a Taylor's series about the a priori position and neglecting higher order terms:

$$\dot{R}^o = \dot{R}(\varphi_0 \lambda_0 B_0) + \frac{\partial \dot{R}}{\partial \varphi} (\varphi - \varphi_0) + \frac{\partial \dot{R}}{\partial \lambda} (\lambda - \lambda_0) + \frac{\partial \dot{R}}{\partial B} (B - B_0) \quad A-13$$

where

$\dot{R}^o$  = the observed range rate (Doppler)

$\dot{R}$  = computed range rate based on current estimate (a priori) of beacon  
(see section 3.1)

$\varphi_0$  = initial geodetic latitude

$\lambda_0$  = initial longitude

$B_0$  = initial estimate of range rate bias

On the first iteration values of  $\phi_0$  and  $\lambda_0$  are generally available to within a few hundred km based on prior knowledge obtained in such ways as crude a priori calculation, satellite field of view and so on. Also on the first iteration the initial guess of the bias  $B_0$  is taken to be zero. The new values of  $\phi$ ,  $\lambda$  and  $B$  obtained after the first iteration are then used as a priori  $\phi_0$ ,  $\lambda_0$  and  $B_0$  for the second iteration. This process is repeated until the solution has converged. The foregoing equations can be rewritten in terms of the 3 variables  $\Delta\phi$ ,  $\Delta\lambda$  and  $\Delta B$ . That is —

$$\Delta\dot{R} = \frac{\partial\dot{R}}{\partial\phi} \Delta\phi + \frac{\partial\dot{R}}{\partial\lambda} \Delta\lambda + \frac{\partial\dot{R}}{\partial B} \Delta B \quad A-14$$

where

$\Delta\dot{R} = \dot{R}_o - \dot{R}$  or residuals which will be minimized as the fit improves

$\Delta\phi = \phi - \phi_0$  = computed adjustment to a priori geodetic latitude

$\Delta\lambda = \lambda - \lambda_0$  = computed adjustment to longitude

$\Delta B = B - B_0$  = computed adjustment to range rate bias ( $B_0$  taken to be zero on first iteration)

In the above  $\dot{R}$  is computed on each iteration based on the current estimate as obtained from the previous iteration — that is,

$$\dot{R} = \frac{(x - S_1) \dot{x} + (y - S_2) \dot{y} + (z - S_3) \dot{z}}{\left[(x - S_1)^2 + (y - S_2)^2 + (z - S_3)^2\right]^{1/2}} + B \quad A-15$$

as before  $x$ ,  $y$ ,  $z$  and  $\dot{x}$ ,  $\dot{y}$ ,  $\dot{z}$ , are the satellite Earth fixed geocentric parameters and  $S_1$ ,  $S_2$ ,  $S_3$  are current beacon coordinates. The first part of the computational problem thus becomes the evaluation of partial derivatives  $\frac{\partial\dot{R}}{\partial\phi}$ ,  $\frac{\partial\dot{R}}{\partial\lambda}$  and  $\frac{\partial\dot{R}}{\partial B}$  which must be computed at the time of each data point collection to

form the overdetermined set of linear equations. In this regard —

$$\frac{\partial \dot{R}}{\partial \phi} = \frac{\partial \dot{R}}{\partial S_1} \frac{\partial S_1}{\partial \phi} + \frac{\partial \dot{R}}{\partial S_2} \frac{\partial S_2}{\partial \phi} + \frac{\partial \dot{R}}{\partial S_3} \frac{\partial S_3}{\partial \phi} \quad A-16$$

$$\frac{\partial \dot{R}}{\partial \lambda} = \frac{\partial \dot{R}}{\partial S_1} \frac{\partial S_1}{\partial \lambda} + \frac{\partial \dot{R}}{\partial S_2} \frac{\partial S_2}{\partial \lambda} \quad A-17$$

$$\frac{\partial \dot{R}}{\partial B} = 1.0 \quad A-18$$

The parts of A-16, A-17, and A-18 which are not a function of the data are:

$$\frac{\partial S_1}{\partial \phi} \doteq -\nu \sin \phi \cos \lambda \quad A-19$$

$$\frac{\partial S_2}{\partial \phi} \doteq -\nu \sin \phi \sin \lambda \quad A-20$$

$$\frac{\partial S_3}{\partial \phi} \doteq \nu (1 - e^2) \cos \phi \quad A-21$$

$$\frac{\partial S_1}{\partial \lambda} = -(\nu + h) \cos \phi \sin \lambda = -S_2 \quad A-22$$

$$\frac{\partial S_2}{\partial \lambda} = (\nu + h) \cos \phi \cos \lambda = S_1 \quad A-23$$

The parts of A-16, A-17, and A-18 which must be computed at each data time are:

$$\frac{\partial \dot{R}}{\partial S_1} = \left[ -\dot{x} + \frac{\dot{R}(x - S_1)}{R} \right] \left[ \frac{1}{R} \right] \quad A-24$$

$$\frac{\partial \dot{R}}{\partial S_2} = \left[ -\dot{y} + \frac{\dot{R}(y - S_2)}{R} \right] \left[ \frac{1}{R} \right] \quad A-25$$

$$\frac{\partial \dot{R}}{\partial S_3} = \left[ -\dot{z} + \frac{\dot{R}(z - S_3)}{R} \right] \left[ \frac{1}{R} \right] \quad A-26$$

In this manner equations A-16, A-17, and A-18 are evaluated at each data time and are used as the basic input to the normal equations which can be written as:

$$\begin{bmatrix} a_{11} & a_{12} & a_{13} \\ a_{21} & a_{22} & a_{23} \\ a_{31} & a_{32} & a_{33} \end{bmatrix} \begin{bmatrix} \Delta \phi \\ \Delta \lambda \\ \Delta B \end{bmatrix} = \begin{bmatrix} c_1 \\ c_2 \\ c_3 \end{bmatrix} \quad A-27$$

or symbolically

$$A \Phi = C$$

$$\Phi = A^{-1} C$$

where for n data points:

$$a_{12} = \sum_{i=1}^n \left( \frac{\partial \dot{R}}{\partial \lambda_i} \right) \left( \frac{\partial \dot{R}}{\partial \phi_i} \right) = a_{21} \quad A-28$$

$$a_{11} = \sum_{i=1}^n \left( \frac{\partial \dot{R}}{\partial \phi_i} \right)^2$$

$$a_{13} = \sum_{i=1}^n \frac{\partial \dot{\mathbf{R}}}{\partial \phi_i} = a_{31}$$

$$a_{22} = \sum_{i=1}^n \left( \frac{\partial \dot{\mathbf{R}}}{\partial \lambda_i} \right)^2$$

$$a_{33} = \sum_{i=1}^n 1 = n$$

$$a_{23} = \sum_{i=1}^n \frac{\partial \dot{\mathbf{R}}}{\partial \lambda_i} = a_{32}$$

ORIGINAL PAGE IS  
OF POOR QUALITY

also

$$c_1 = \sum_{i=1}^n \frac{\partial \dot{\mathbf{R}}}{\partial \phi_i} \Delta \dot{\mathbf{R}}_i$$

$$c_2 = \sum_{i=1}^n \frac{\partial \dot{\mathbf{R}}}{\partial \lambda_i} \Delta \dot{\mathbf{R}}_i$$

$$c_3 = \sum_{i=1}^n \Delta \dot{\mathbf{R}}_i$$

As the microcomputer steps through the data, which has first been stored in RAM, it pauses at each data line and computes the partial derivatives and range rate residuals and places the result in temporary storage. Each data point requires less than 1 second of computation time. Once the microcomputer

has processed all data it computes the sums indicated in A-28 which correspond to the scalar constants  $a_{11}$  through  $a_{33}$  and  $c_1, c_2, c_3$ , of A-27. Equation A-27 is then solved for  $\Delta\phi, \Delta\lambda$  and  $\Delta B$  thus obtaining a solution for beacon location and frequency (range rate) bias. This takes less than 10 seconds. The new values of  $\phi, \lambda$  and  $B$  are then used as an a priori for the next iteration and so on. Although this particular microcomputer was programmed to determine latitude and longitude of stationary or slowly moving beacons using one or two Doppler data spans, the extension to moving beacons and height recovery is also being investigated. If a sufficient quantity of Doppler data is available it is in principle a simple step to modify the foregoing equations to handle additional unknowns.

## ACKNOWLEDGEMENT

The authors wish to thank P. D. Argentiero, R. Garza-Robles, D. W. Koch, E. R. Lancaster, and J. W. Marini of the NASA-GSFC Measurements Evaluation Branch, who provided invaluable assistance in the form of supporting analysis and critical review regarding the algorithms discussed in this paper. Also greatly acknowledged is the complete cooperation of C. P. Ashcraft and C. H. Vermillion of the NASA-GSFC Sensor Evaluation Branch, who made available their NIMBUS-6 telemetry receiving station for use during the real-time phase of the microcomputer position location tests.

## REFERENCES

1. Green, T., "Satellite Doppler Data Processing for Platform Navigation", IEEE Transactions on Geoscience Electronics, Vol. GE-13, No. 1, January 1975.
2. Coates, J. L., "The NIMBUS-F Random Access Measurement System (RAMS)", IEEE Transactions on Geoscience Electronics, Vol. GE-13, Nr. 1, January 1975.
3. Cote, C., and P. Julian, "The Tropical Wind Energy Conversion and Reference Level Experiment (TWERLE)" as presented in "The NIMBUS-6 User's Guide" NASA-GSFC February 1975.
4. Schmid, P. E., J. J. Lynn, and F. O. Vonbun, "Single Pass Doppler Positioning for Search and Rescue Missions", Proceedings of IEEE 1976 Position Location and Navigation Symposium, 1-3 November 1976.
5. Brandel, D. L., P. E. Schmid, and B. J. Trudell, "Improvements in Search and Rescue Distress Alerting and Locating Using Satellites", IEEE WESCON, Sept. 14-17, 1976.
6. Lynn, J. J. and P. E. Schmid, "Remote Beacon Location from a Single Satellite Pass", COSPAR Tel-Aviv, Israel, 7-18 June 1977.
7. Marini, J. W., "Initial Position Estimates for Satellite-Aided Search and Rescue", NASA-GSFC X-932-76-245, October 1976.
8. Filipowsky, R. F. and E. I. Muehldorf, "Space Communications Systems", p. 42-49, Prentice Hall, Englewood Cliffs, N.J., 1965.
9. Marini, J. W., "Tropospheric Range-Rate Tracking Data Correction", NASA-GSFC X-551-72-277, August 1972.
10. Saxton, J. A., "Advances in Radio Research", Vol. 1, Academic Press, New York, 1964.

11. Bean, B. R. and E. J. Dutton, "Radio Meteorology", National Bureau of Standards Monograph 92, 1966.
12. Schmid, P. E., R. B. Bent, S. K. Llewellyn, G. Nestorczuk and S. Rangaswamy, "NASA-GSFC Ionospheric Corrections to Satellite Tracking Data," NASA-GSFC X-591-73-281, December 1973.
13. Schmid, P. E., "The Feasibility of a Direct Relay of Apollo Spacecraft Data Via A Communication Satellite", NASA TN D-4048, August 1967.
14. Koch, D. W., "Error Analysis for Satellite Aided Search and Rescue", NASA-GSFC X-932-76-86, August 1976.
15. Kershner, R. B., "The Doppler Concept and the Operational Navy Navigation System", p. 5-24 in Satellite Doppler Positioning Vol. 1, Proceedings International Geodetic Symposium, Las Cruces, New Mexico, October 1976.
16. Holton, W. C., "The Large-Scale Integration of Microelectronic Circuits", Scientific American, p. 82-94, special issue on "Microelectronics", September 1977.
17. Hodges, D. A., "Microelectronic Memories", p. 130-145, Scientific American, special issue on "Microelectronics", September 1977.
18. Hilburn, J. L. and P. M. Julich, "Microcomputers/Microprocessors: Hardware, Software and Applications", Prentice-Hall, Inc. Englewood Cliffs, N.J., 1976.
19. Waite, M. and M. Pardee, "Microcomputer Primer", Howard W. Sams & Co., Indianapolis, Indiana, 1976.
20. MOS Technology Inc., "MCS6500 Microcomputer Family Hardware Manual", January 1976.

21. Kaula, W. M., "Theory of Satellite Geodesy", Chapter 4, Geometry of Satellite Observations, Blaisdell Publishing Co., Waltham, Massachusetts, 1966.
22. Argentiero, P. and R. Garza-Robles, "Efficient Estimation Algorithms for a Satellite-Aided Search and Rescue Mission", NASA-GSFC X-932-77-194, August 1977.
23. Hartwell, J. G., F. M. Loveless, G. E. Morduch, "A Photogrammetric and Tracking Network Analysis Program", ETL-CR-73-17, October 1973, Old Dominion Systems, Inc., prepared for U.S. Army Engineer Topographic Laboratories, Fort Belvoir, Virginia.
24. Wylie, C. R. Jr., "Advanced Engineering Mathematics", p. 527-541, McGraw-Hill, New York, 1951.

1. Report No. TM78046	2. Government Accession No.	3. Recipient's Catalog No.	
4. Title and Subtitle Satellite Doppler Data Processing Using A Microcomputer		5. Report Date December 1977	
		6. Performing Organization Code	
7. Author(s) P. E. Schmid and J. J. Lynn		8. Performing Organization Report No.	
9. Performing Organization Name and Address NASA-Goddard Space Flight Center Greenbelt, Maryland 20771		10. Work Unit No.	
		11. Contract or Grant No.	
12. Sponsoring Agency Name and Address N/A		13. Type of Report and Period Covered Technical Memorandum December 1977	
		14. Sponsoring Agency Code	
15. Supplementary Notes To be published in IEEE Transactions on Aerospace and Electronic Systems (AES)			
16. Abstract  This paper describes a microcomputer which was developed to compute ground radio beacon position locations using satellite measurements of Doppler frequency shift. Both the computational algorithms and the microcomputer hardware incorporating these algorithms are discussed. Results are presented where this microcomputer in conjunction with the NIMBUS-6 Random Access Measurement System (RAMS) provides real-time calculation of beacon latitude and longitude.			
17. Key Words (Selected by Author(s)) Microcomputer, Satellite Doppler, Position Location		18. Distribution Statement	
19. Security Classif. (of this report) U	20. Security Classif. (of this page) U	21. No. of Pages	22. Price*